

SJD-PAC: Accelerating Speculative Jacobi Decoding via Proactive Drafting and Adaptive Continuation

Jialiang Kang¹ Han Shu² Wenshuo Li² Yingjie Zhai² Xinghao Chen^{2*}

¹Peking University

²Huawei Technologies

jkang@stu.pku.edu.cn

{han.shu, liwenshuo, zhaiyingjie, xinghao.chen}@huawei.com

Abstract

Speculative Jacobi Decoding (SJD) offers a draft-model-free approach to accelerate autoregressive text-to-image synthesis. However, the high-entropy nature of visual generation yields low draft-token acceptance rates in complex regions, creating a bottleneck that severely limits overall throughput. To overcome this, we introduce SJD-PAC, an enhanced SJD framework. First, SJD-PAC employs a proactive drafting strategy to improve local acceptance rates in these challenging high-entropy regions. Second, we introduce an adaptive continuation mechanism that sustains sequence validation after an initial rejection, bypassing the need for full resampling. Working in tandem, these optimizations significantly increase the average acceptance length per step, boosting inference speed while strictly preserving the target distribution. Experiments on standard text-to-image benchmarks demonstrate that SJD-PAC achieves a $3.8\times$ speedup with lossless image quality.

1. Introduction

Autoregressive (AR) models for text-to-image (T2I) synthesis [1, 2, 14, 18, 21, 27–30] have achieved state-of-the-art generation quality, rivaling top-tier diffusion models. These models discretize images into token sequences using a Vector Quantizer (VQ) [3] and frame generation as a sequence-to-sequence problem [30]. However, their primary drawback is severe inference latency, as generating a high-resolution image requires sequentially predicting thousands of tokens [18, 22].

Speculative Decoding (SD) [9, 11, 17] accelerates AR models by using a small, fast *draft* model to propose token sequences, which a large *target* model then verifies in parallel. While effective in other domains, this approach requires

training and maintaining a separate draft model. More critically, standard SD techniques are largely ineffective for T2I generation [9]. For instance, EAGLE [12], despite its success in accelerating Large Language Models (LLMs), yields negligible speedups for T2I models [9].

This failure stems from the high-entropy nature of T2I generation. In LLMs, high sampling temperatures increase output entropy and significantly degrade the SD acceptance rate [16]. T2I models inherently exhibit this high entropy even at standard sampling temperatures [31]. Intuitively, this means many tokens are nearly equally plausible, making it difficult for a draft model to accurately anticipate the target model’s predictions.

Speculative Jacobi Decoding (SJD) [22] offers a compelling alternative. It is both training-free and lossless, rigorously preserving the target model’s output distribution. SJD re-frames generation as a fixed-point iteration, using the output distribution from the previous iteration p^{t-1} as the draft for the current iteration p^t . Despite its elegance, SJD typically yields only a modest $\sim 2\times$ speedup, which remains insufficient to make AR models latency-competitive.

To understand this limitation, we analyze SJD’s practical performance by examining the distribution of accepted tokens per forward step. As shown in Fig. 1a, this distribution is highly skewed and long-tailed. In nearly 50% of forward passes, SJD accepts only a single token. This occurs when the first draft token fails verification, triggering a resample and yielding zero acceleration for that step. Consequently, as Fig. 1b illustrates, these single-token steps contribute nothing to the overall speedup (which is derived solely from extra accepted tokens, i.e., acceptance length > 1). The average $\sim 2\times$ speedup is thus disproportionately driven by a small fraction of steps that successfully accept numerous tokens in a single pass.

This observation naturally raises two critical questions:

1. **Mitigating Low-Efficiency Steps:** How can we reduce the frequency of single-token acceptances to minimize

*Corresponding author.

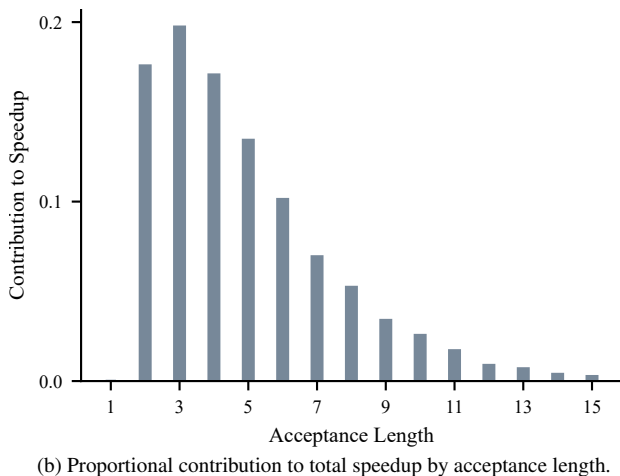
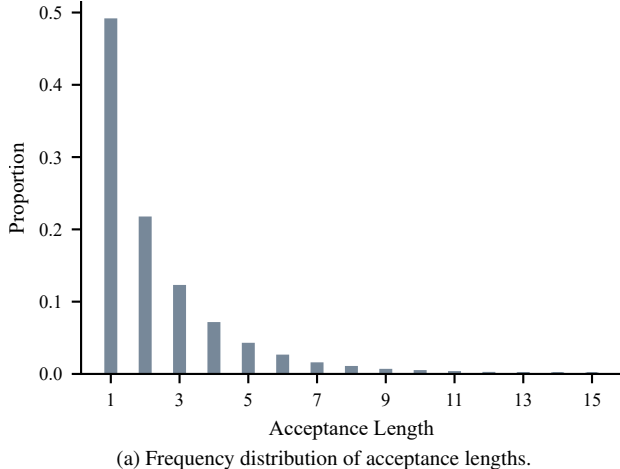


Figure 1. Analysis of acceptance lengths in SJD [22]. The speedup shown in (b) is derived entirely from additionally accepted tokens (acceptance length > 1).

their drag on overall speedup?

2. **Maximizing Acceptance Length:** How can we increase the number of successfully verified tokens in a single pass to amplify their contribution to acceleration?

In this paper, we propose SJD-PAC, an enhanced SJD framework that directly addresses both challenges. Crucially, SJD-PAC is entirely training-free and rigorously lossless.

To *mitigate low-efficiency steps*, we introduce **Proactive Drafting (PD)**. This strategy targets the root cause of single-token acceptances: the context mismatch caused by a rejection. When a token at position i is rejected, the context for all subsequent proposals $x_{j>i}$ becomes invalid, often triggering cascading rejections in the subsequent iteration. PD addresses this by modifying the drafting phase. Instead of proposing a single sequence, PD proactively constructs multiple diverse proposal paths rooted at the newly

resampled position. By providing several alternatives, PD increases the likelihood that at least one path remains valid during verification, directly suppressing the spike in single-token acceptances.

To *maximize acceptance length*, we introduce **Adaptive Continuation (AC)**. This technique modifies the standard SJD verification loop, which typically terminates upon the first rejection. AC, in contrast, eliminates this hard termination. When a rejection occurs at position i , AC resamples only the failed token x_i^t and continues the verification process for all subsequent positions $j > i$. This mechanism allows AC to preserve valid tokens beyond the initial point of failure, discarding only the rejected ones. This creates a more stable initial state for the next Jacobi iteration while maintaining rigorous losslessness.

Our main contributions are as follows:

- We identify and analyze the skewed acceptance-length distribution of SJD in T2I models, pinpointing it as the primary performance bottleneck.
- We introduce SJD-PAC, a novel, training-free, and lossless SJD variant incorporating two new techniques: Proactive Drafting (PD) to mitigate cascading rejections, and Adaptive Continuation (AC) to preserve valid tokens beyond the initial failure.
- We empirically demonstrate that SJD-PAC achieves state-of-the-art acceleration for lossless T2I generation, significantly outperforming the original SJD [22] and recent lossy alternatives [19, 23].

2. Related Works

2.1. Autoregressive Text-to-Image Generation

Early autoregressive T2I models [18] utilized a two-stage pipeline. First, an image tokenizer, such as a VQ-VAE [24], discretized the image into a 1D sequence of tokens. A large decoder-only Transformer [25] then generated this sequence autoregressively, conditioned on a text prompt. Parti [30] exemplified this paradigm, scaling the Transformer to billions of parameters to achieve high-fidelity synthesis. More recently, the field has shifted toward unified, end-to-end architectures [1, 2, 14, 21, 27–29]. By jointly co-training the tokenizer and Transformer on vast mixed-modal datasets within a single framework, these models build a richer contextual understanding and achieve state-of-the-art generation quality. Despite these architectural advancements, the fundamental autoregressive bottleneck remains: tokens must be generated sequentially during inference, resulting in significant latency.

2.2. Speculative Decoding

Speculative Decoding (SD) [11] has emerged as an effective acceleration strategy for Large Language Models (LLMs). It typically employs a small draft model to generate candi-

date tokens, which are subsequently verified in parallel by a large target model. This core concept has been widely extended: SpecInfer [15] utilizes tree-based drafting for more efficient verification, while ViSpec [10] adapts the principle for Vision-Language Models (VLMs).

In the context of T2I models, LANTERN [9] addresses the inherently low acceptance rates of image tokens by proposing a relaxed SD framework that accepts plausible, albeit non-identical, proposals. LANTERN++ [17] further enhances this approach using static tree drafting. Concurrently, a distinct, training-free paradigm was introduced with Speculative Jacobi Decoding (SJD) [22]. SJD leverages a fixed-point iteration mechanism, enabling the target model to generate its own drafts. This achieves lossless acceleration without requiring an auxiliary draft model. Subsequent methods, such as Grouped Speculative Decoding (GSD) [19] and SJD2 [23], have explored variations of this approach, though often at the cost of reintroducing training requirements or compromising the lossless guarantee.

While some relaxed SD approaches operate on the premise that substituting specific tokens with similar alternatives does not necessarily degrade perceptual quality [19], image generation can be exceedingly sensitive to token-level perturbations. As illustrated in Fig. 2, modifying a single token during generation can introduce severe visual artifacts into the final output. Consequently, maintaining a lossless guarantee remains critical for the reliable application of SD in T2I models.

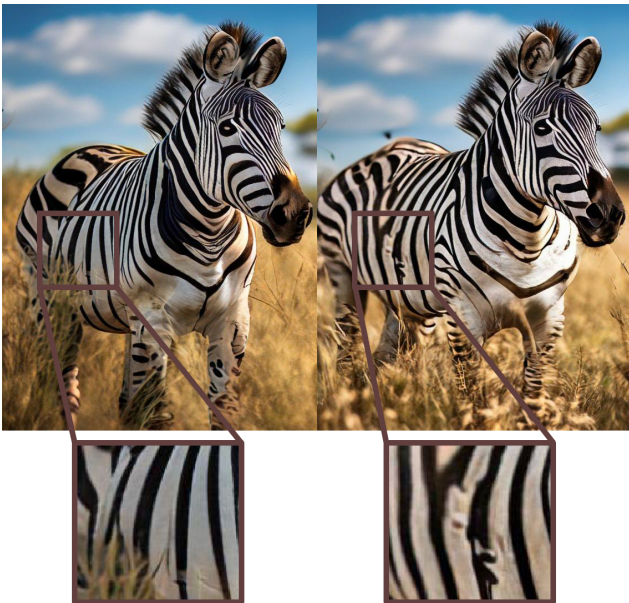


Figure 2. High sensitivity of AR T2I models to token perturbations. **Left:** Original generation. **Right:** Replacing a single token (0.04% of total tokens) during the autoregressive process causes a severe visual artifact (red box).

3. Preliminaries

3.1. Notations

In this paper, we denote the target T2I model to be accelerated as M . Let $p(\cdot | \cdot)$ be its output probability distribution. A proposal distribution $q(\cdot | \cdot)$ is used to generate draft tokens. If a separate draft model is utilized, q represents its output distribution; in training-free methods like SJD [22], q is the distribution derived from cached, stale logits from a previous iteration of M . We use lowercase for individual tokens, e.g., x , and uppercase for sequences, e.g., X . Subscripts denote token positions and superscripts denote iterations; thus, x_i^t is the token at position i in iteration t . We use $X_{i:j}$ to represent the subsequence (x_i, \dots, x_j) and $X_{<i}$ for the prefix (x_1, \dots, x_{i-1}) .

3.2. Rejection Sampling

Rejection sampling [26] is a Monte Carlo method for drawing samples from a target distribution p using a proposal distribution q . The technique guarantees that accepted samples are distributed exactly according to p , provided that $p(x) \leq c \cdot q(x)$ holds for all x and a known constant $c \geq 1$. Crucially, p and q are not required to be conditional on the same context or prefix [22, 26]. In speculative decoding, a sample $x \sim q$ is drawn and accepted if $u \leq p(x)/q(x)$, where $u \sim U(0, 1)$. If x is rejected, a new token is sampled from the normalized residual distribution $p'_{\text{res}}(x) \propto \max(p(x) - q(x), 0)$. For brevity, we will henceforth use $\max(p(x) - q(x), 0)$ to denote this calibrated distribution, omitting the normalization factor.

3.3. Speculative Jacobi Decoding

SJD [22] treats AR generation as a fixed-point iteration problem. It operates on a token sequence $X = (x_1, \dots, x_L)$ within a fixed-length Jacobi window of size L . At the start of iteration t , the inputs are the token sequence X^{t-1} and its corresponding stale output distributions $P^{t-1} = M(X^{t-2})$ cached from the previous iteration. A single forward pass on X^{t-1} yields the new target distributions $P^t = M(X^{t-1})$.

The core SJD verification loop then proceeds sequentially from $i = 1$ to L . At each position i :

1. **Target distribution:** $p_i = P^t(\cdot | X_{<i}^{t-1})$.
2. **Proposal distribution:** $q_i = P^{t-1}(\cdot | X_{<i}^{t-2})$.
3. **Draft token:** x_i^{t-1} , generated in the previous iteration.
4. **Verification:** x_i^{t-1} is accepted or rejected via rejection sampling using p_i and q_i .

If x_i^{t-1} is accepted, we set $x_i^t \leftarrow x_i^{t-1}$ and proceed to position $i + 1$. If x_i^{t-1} is rejected, a new token x_i^t is sampled from the calibrated distribution $\max(p_i - q_i, 0)$, and the verification loop terminates. Following termination at position i , the remaining tokens $X_{i+1:L}^t$ are sampled

from their respective target distributions $p_j(\cdot | X_{<j}^{t-1})$ for $j = i + 1, \dots, L$. Finally, i new tokens are initialized and appended to maintain the window size L , and the process advances to iteration $t + 1$.

4. Method

While SJD [22] is efficient and lossless, our analysis in Sec. 1 reveals that its performance is bottlenecked by frequent rejections and short acceptance lengths. In this section, we introduce our proposed method, SJD-PAC, which incorporates two key innovations: Proactive Drafting (PD) and Adaptive Continuation (AC). These techniques work synergistically to reduce the frequency of rejections and increase the number of tokens accepted per forward pass, thereby enhancing overall generation speed without sacrificing output quality. A conceptual illustration of how PD and AC modify the standard SJD rejection process is provided in Fig. 3.

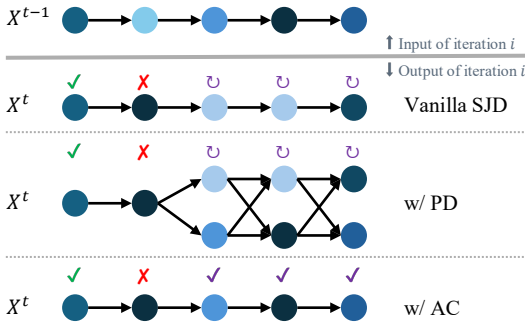


Figure 3. A conceptual overview of our proposed components compared to Vanilla SJD, illustrating how each method handles a token rejection (red \times) at iteration t . **Vanilla SJD (Top)**: A rejection at position 2 forces a break, and the entire subsequent sequence is resampled (purple \circ). **w/ PD (Middle)**: After a rejection, Proactive Drafting builds a diverse K -ary tree at the rejection point to increase the probability of acceptance in the subsequent iteration. **w/ AC (Bottom)**: After a rejection, Adaptive Continuation *continues* the verification loop, preserving subsequent valid tokens (purple \checkmark) instead of terminating.

4.1. Proactive Drafting (PD)

To **mitigate low-efficiency steps**, specifically the frequent single-token acceptances, we first modify the *proposal generation* process that follows a rejection. In standard SJD [22], a rejection at position i during iteration t creates a context mismatch. After the new token x_i^t is resampled, the standard SJD procedure generates the remainder of the sequence $X_{i+1:L}^t$ by sampling from the target distributions $p_j(\cdot | X_{<j}^{t-1})$, where $j = i + 1, \dots, L$. The problem is that these distributions are conditioned on a stale prefix $X_{<j}^{t-1}$, which contains the rejected token x_i^{t-1} rather than the corrected x_i^t . Consequently, this new proposal $X_{i+1:L}^t$ is mis-

aligned with its own context. When used as the draft in the next iteration $t + 1$, the tokens $X_{i+1:L}^t$ are highly likely to be rejected immediately at $i + 1$, leading to a cascading spike of single-token acceptances.

PD addresses this by proactively constructing a new, more diverse proposal X^t the moment a rejection occurs at i . After the new token x_i^t is resampled, we build this new proposal rooted at x_i^t :

- Shallow, Wide Tree:** For positions j from $i + 1$ to $i + D$ (e.g., $D = 3$), we sample K candidate tokens (e.g., $K = 4$) without replacement from the target distribution $p(\cdot | X_{<j}^{t-1})$. This forms a K -ary tree of depth D , providing a diverse set of local candidates.
- Chain Extension:** For all subsequent positions $j > i + D$, we extend one of these paths (e.g., the first path, $k = 1$) as a single proposal chain up to the full length L , by sampling autoregressively from $p(\cdot | X_{<j}^{t-1})$.

This new hybrid proposal, a shallow tree followed by a long chain, is then fed into iteration $t + 1$. By providing K diverse options at the critical, post-rejection local boundary, PD increases the likelihood that at least one path will remain valid, directly mitigating the single-token acceptance spike. Unlike tree-based speculative decoding [15], our tree is built only locally and is conditioned on the potentially stale context X^{t-1} . This avoids the need for multiple model forward passes.

4.2. Adaptive Continuation (AC)

To **maximize the acceptance length**, we modify the verification loop of standard SJD. In SJD, the verification at iteration t terminates upon the first rejection at position i , discarding all subsequent proposal tokens $X_{i+1:L}^{t-1}$. This is inefficient, as many tokens might remain valid under the shifted context. Adaptive Continuation (AC) eliminates this hard break statement. Upon a rejection at i , AC resamples $x_i^t \sim \max(p_i - q_i, 0)$ and continues verifying the remaining positions $j = i + 1, \dots, L$.

For $j > i$, the updated prefix $X_{<j}^t$ renders the pre-computed draft and target distributions (p_j, q_j) stale. Re-computing them would negate the speedup. However, utilizing these stale distributions remains highly effective due to the strong *locality* of image tokens. To empirically validate this, we use MS-COCO [13] and prompt Lumina-mGPT [14] to generate both images and text stories. By individually masking the KV-cache at a preceding position with an offset j (i.e., at position $i - j$), we measure the Total Variation (TV) distance of the output distribution at position i before and after the perturbation. As shown in Fig. 4, the TV distance d_{TV} for image tokens rapidly approaches zero as the distance from the perturbed context increases. This contrasts sharply with text generation, which remains highly sensitive to distant context changes.

Since the acceptance probability of a single draft token

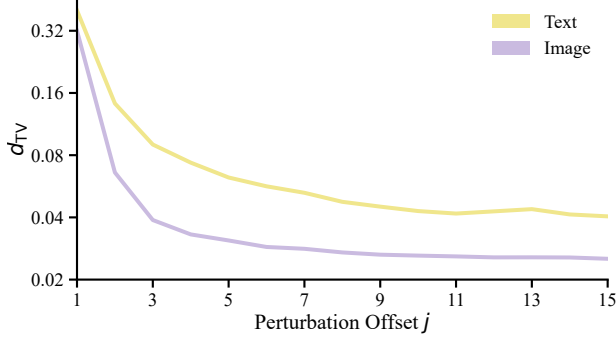


Figure 4. Total Variation distance d_{TV} for text and image generation with respect to the perturbation offset j .

is $1 - d_{TV}(p, q)$ [20], standard rejection sampling naturally preserves tokens when d_{TV} is low. Specifically, the probability that a token at position i remains unchanged is $1 - d_{TV}(p_i^{t-1}, p_i^t)$. In contrast, if SJD were to independently resample the same token, the probability would be $\sum_{\mathcal{V}} p_i^{t-1} p_i^t \leq \exp\left(-\frac{H_2(p^{t-1}) + H_2(p^t)}{2}\right)$, where H_2 denotes the order-2 Rényi entropy [4]. Given the high entropy of image distributions, this resampling probability is negligible (< 0.01). By evaluating the remaining tokens using the stale distributions (p_j, q_j) via standard rejection sampling, AC effectively exploits the asymptotic behavior observed in Fig. 4 to maximize token retention, achieving a retention probability > 0.7 :

- **Acceptance:** Set $x_j^t \leftarrow x_j^{t-1}$, preserving the token.
- **Rejection:** Sample a new token $x_j^t \sim \max(p_j - q_j, 0)$.

This process yields a full-length sequence X^t with minimal deviation from X^{t-1} , providing a stable initialization for iteration $t + 1$. Crucially, AC remains rigorously lossless. The tail sequence $X_{>i}^t$, although generated using stale distributions, serves only as the draft for the next iteration, where it will be verified against updated, exact target distributions.

4.3. Full Algorithm

Our full algorithm, SJD-PAC, is detailed in Algorithm 1. It integrates the two aforementioned components: Adaptive Continuation (AC) and Proactive Drafting (PD). The algorithm begins by performing a parallel forward pass to obtain the target probabilities P^t (Line 2). We initialize a variable `first_rej_idx` to track the position of the first mismatch (Line 4).

In the AC Loop (Lines 5–17), unlike standard SJD which terminates on the first rejection, our loop always continues to verify all L tokens. During this pass, standard acceptance (Line 10) or rejection sampling (Line 12) is performed for each token. If a token is rejected, we check if it is the first rejection; if so, we record its position in `first_rej_idx` (Lines 13–15) and continue the loop without breaking.

Algorithm 1 SJD-PAC (Ours)

```

1:  $X^{t-1}$ : draft tokens,  $P^{t-1}$ : draft probs
2:  $P^t \leftarrow \text{PARALLELFORWARD}(X^{t-1})$ 
3:  $X^t \leftarrow []$ 
4: first_rej_idx  $\leftarrow -1$ 
5: for  $i = 1 \rightarrow L$  do ▷ Adaptive Continuation Loop
6:    $p_i \leftarrow P_i^t$ ;  $q_i \leftarrow P_i^{t-1}$ ;  $x_i^{t-1} \leftarrow X_i^{t-1}$ 
7:    $r \sim U[0, 1]$ 
8:   if  $r < \min(1, \frac{p_i}{q_i})$  then
9:      $x_i^t \leftarrow x_i^{t-1}$  ▷ Accept
10:  else
11:     $x_i^t \leftarrow \text{SAMPLE}(\max(p_i - q_i, 0))$  ▷ Reject
12:    if first_rej_idx =  $-1$  then
13:      first_rej_idx  $\leftarrow i$ 
14:    end if
15:  end if
16: end for ▷ No break
17: if first_rej_idx  $\neq -1$  then ▷ Proactive Drafting
18:    $X^t \leftarrow \text{PD}(X^t, \text{first\_rej\_idx})$ 
19: end if
20: return  $X^t, P^t$ 

```

After the loop, we check if any rejections occurred (Line 19). If `first_rej_idx` is not -1 , we activate the Proactive Drafting (PD) mechanism (Line 20). The PD function leverages the target distribution p to generate diversified token sequences starting from the position of the first rejection.

SJD-PAC is rigorously lossless, as both the AC and PD components preserve the underlying target distribution. The framework is also training-free and model-agnostic.

5. Experiments

5.1. Experimental Setup

Models and Benchmarks. We evaluate our method on two text-to-image models: Lumina-mGPT [14] and Emu3 [27]. For Lumina-mGPT, we use the standard 7B model at a 768×768 resolution. Emu3 is an 8B model that generates 720×720 images. Following standard practice [14], we use a top-2000 logit sampler, a temperature of 1, and a classifier-free guidance (CFG) weight of 3 for inference. We conduct evaluations on two standard benchmarks: the MS-COCO 2017 validation set [13] and the PartiPrompts dataset [5].

Baselines and Implementation. We compare SJD-PAC against several strong decoding baselines. These include lossless methods, namely EAGLE-2 [12] and Speculative Jacobi Decoding (SJD) [22], as well as high-performing lossy methods, including LANTERN++ [17], GSD [19], and SJD2 [23]. Our implementation of EAGLE-2 is adapted

from the LANTERN codebase [9]. For all other baselines, we use the official parameters and checkpoints from their respective papers. To ensure a fair comparison, if our reproduced metric for a baseline falls below its reported score, we report the published value. For our method, we use a draft tree with depth $D = 3$ and $K = 4$ branches per node, and set the verification window size to $L = 64$.

Evaluation Metrics. We evaluate both generation quality and decoding efficiency. **Quality:** We use the Fréchet Inception Distance (FID) [4, 7] and CLIP-Score [6, 8] to assess visual fidelity. Both metrics are reported on the MS-COCO validation set. Since the PartiPrompts dataset lacks ground-truth images, we report only the CLIP-Score for this benchmark. **Speed:** We report two metrics.

- **Step Compression Ratio**, defined as:

$$S = \frac{\text{generated tokens}}{\text{decoding steps}},$$

which measures theoretical acceleration.

- **End-to-end Speedup**, which measures the practical wall-clock speedup against standard autoregressive decoding.

5.2. Main Results

Table 1 presents the main speed and quality comparisons on the MS-COCO 2017 [13] and PartiPrompts [5] datasets using Lumina-mGPT [14] and Emu3 [27]. As shown in the table, SJD-PAC achieves state-of-the-art acceleration across all configurations while rigorously maintaining baseline image quality.

For Lumina-mGPT, SJD-PAC achieves the highest acceleration, recording a $4.51\times$ step compression and a $3.80\times$ wall-clock speedup on MS-COCO. This significantly surpasses other lossless methods like EAGLE [12] ($2.10\times$) and SJD [22] ($2.05\times$). Crucially, this speedup incurs zero quality degradation: our FID and CLIP-Score are virtually identical to the original model (30.69 vs. 30.79 and 31.21 vs. 31.31, respectively). Notably, our lossless acceleration even exceeds that of lossy counterparts. For instance, while GSD [19] achieves a $3.62\times$ latency speedup, it suffers a notable quality drop (33.12 FID). In contrast, SJD-PAC is demonstrably faster ($3.80\times$) while preserving high fidelity.

The results on Emu3 [27] reinforce this trend. SJD-PAC again achieves the highest speedup among all lossless methods ($3.25\times$ on MS-COCO) while preserving the baseline generation quality (FID: 31.10 vs. 31.12). Although SJD2 reports a higher step compression ratio ($5.62\times$), it requires double our window length (128 vs. 64). This introduces significant computational overhead that limits its practical acceleration, resulting in a much lower wall-clock speedup ($2.54\times$).

We observe a consistent pattern on the PartiPrompts dataset. For both Lumina-mGPT and Emu3, SJD-PAC delivers the best lossless wall-clock speedup ($3.97\times$ and $3.51\times$, respectively) and the highest step compression in the lossless category. Across all cases, our method preserves the baseline CLIP-Score, outperforming methods like LANTERN++ [17], GSD [19], and SJD2 [23], which all exhibit quality degradation. While the lossy GSD [19] posts a high latency speedup ($4.65\times$) on Lumina-mGPT, SJD-PAC ($3.97\times$) remains highly competitive without the associated quality drop (our 32.07 vs. GSD’s 31.25).

These quantitative results demonstrate that SJD-PAC establishes a new state-of-the-art. It outperforms all existing lossless techniques in both step reduction and latency speedup, yielding acceleration competitive with lossy methods, all without compromising the foundation model’s generation quality.

5.3. Ablation Study

This section presents an ablation study evaluating our proposed components, Proactive Drafting (PD) and Adaptive Continuation (AC), along with the key hyperparameters of the PD mechanism. All experiments use the Lumina-mGPT model on the MS-COCO dataset.

5.3.1. Effectiveness of Proposed Components

We incrementally add our components to the SJD baseline to quantify their impact, as shown in Tab. 2. The baseline SJD with a window length $L = 32$ achieves $2.31\times$ step compression. Integrating Proactive Drafting (PD) increases this to $2.71\times$, highlighting the benefit of drafting a K -ary tree over a simple chain, which allows for more potential acceptance paths. Adding Adaptive Continuation (AC), which stabilizes the sequence after rejections (see Sec. 4.2), further improves compression to $3.52\times$.

With AC equipped, the $L = 32$ window becomes a bottleneck as tokens stabilize faster. Expanding the window length to $L = 64$ fully leverages our method, achieving our main result of $4.51\times$ step compression. While larger window sizes ($L > 64$) yield marginal gains, they incur significant computational overhead that negates practical speedups on our hardware. Therefore, we select $L = 64$ as the optimal default to balance efficiency and speed. These results confirm that both PD and AC are crucial for performance.

5.3.2. Proactive Drafting Hyperparameters

We investigate the two key hyperparameters of PD: the K -ary factor K and the tree depth D . As shown in Tab. 3, when fixing $D = 3$, increasing K from 2 to 4 yields consistent improvements ($4.23\times$ to $4.51\times$). However, performance slightly drops at $K = 5$ ($4.47\times$). Similarly, when fixing $K = 4$, $D = 3$ ($4.51\times$) outperforms both a shallower $D = 2$ ($4.34\times$) and a deeper $D = 4$ ($4.49\times$).

Table 1. Main results comparing our SJD-PAC method against baselines on acceleration and image quality. We report Step Compression (\uparrow), wall-clock Latency speedup (\uparrow), FID (\downarrow), and CLIP-Score (\uparrow) on the Lumina-mGPT and Emu3 models. Evaluations are conducted on the MS-COCO 2017 and PartiPrompts benchmarks. **Bold** indicates the highest speedups in each category.

Configuration	Training-Free	Lossless	Acceleration (\uparrow)		Image Quality	
			Step	Latency	FID (\downarrow)	CLIP-Score (\uparrow)
MS-COCO 2017						
Lumina-mGPT [14]	✓	✓	1.00×	1.00×	30.79	31.31
w/ EAGLE [12]	✗	✓	2.94×	2.10×	30.68	31.73
w/ SJD [22]	✓	✓	2.22×	2.05×	31.13	31.33
w/ LANTERN++ $_{k=10, \lambda=2}$ [17]	✗	✗	3.19×	2.28×	29.96	30.11
w/ GSD $_{G=10}$ [19]	✓	✗	3.39×	3.62×	33.12	31.25
w/ SJD2 [23]	✗	✗	4.02×	2.81×	31.40	31.80
w/ SJD-PAC (Ours)	✓	✓	4.51×	3.80×	30.69	31.21
<hr/>						
Emu3 [27]	✓	✓	1.00×	1.00×	31.12	31.05
w/ SJD [22]	✓	✓	2.32×	2.01×	30.74	30.95
w/ SJD2 [23]	✗	✗	5.62×	2.54×	31.50	30.40
w/ SJD-PAC (Ours)	✓	✓	4.31×	3.25×	31.10	30.99
<hr/>						
PartiPrompts						
Lumina-mGPT [14]	✓	✓	1.00×	1.00×	-	32.01
w/ EAGLE [12]	✗	✓	2.86×	2.01×	-	32.01
w/ SJD [22]	✓	✓	2.28×	2.13×	-	32.06
w/ LANTERN++ $_{k=10, \lambda=2}$ [17]	✗	✗	3.02×	2.10×	-	31.07
w/ GSD $_{G=50}$ [19]	✓	✗	3.76×	4.65×	-	31.25
w/ SJD2 [23]	✗	✗	3.82×	2.51×	-	31.54
w/ SJD-PAC (Ours)	✓	✓	4.62×	3.97×	-	32.07
<hr/>						
Emu3 [27]	✓	✓	1.00×	1.00×	-	31.85
w/ SJD [22]	✓	✓	2.35×	2.11×	-	31.65
w/ SJD2 [23]	✗	✗	4.72×	2.04×	-	31.23
w/ SJD-PAC (Ours)	✓	✓	4.59×	3.51×	-	31.87

Table 2. Ablation study on the contribution of each component (PD, AC) and the effect of window length (L).

Method	Window Len	Step Compression (\uparrow)
Baseline	32	2.31×
+ PD	32	2.71×
+ PD + AC	32	3.52×
+ PD + AC	64	4.51×

This trade-off occurs because the total number of verified tokens per step, i.e., the computational budget, is fixed in this setup. Allocating more tokens to the drafting tree by increasing K or D inherently shortens the subsequent drafting chain. Maintaining this fixed budget prevents the computational overhead from becoming compute-bound—an issue that diminishes wall-clock acceleration in methods like SJD2 [23] due to excessively long windows (see Sec. 5.2).

Consequently, we identify $K = 4, D = 3$ as the optimal configuration.

Table 3. Hyperparameter sensitivity analysis for Proactive Drafting’s K -ary factor (K) and tree depth (D). All experiments use the full method with $L = 64$.

K	D	Step Compression (\uparrow)
2	3	4.23×
3	3	4.42×
5	3	4.47×
4	2	4.34×
4	4	4.49×
4	3	4.51×



Figure 5. **Qualitative Comparison.** Images generated using various prompts from the MS-COCO dataset [13]. The outputs from our accelerated method (SJD-PAC) are visually indistinguishable from those of the baseline models, corroborating our lossless guarantee.

5.4. Visual Inspection

Because SJD-PAC is algorithmically lossless, it theoretically guarantees the preservation of image quality. This is visually supported by samples generated from the MS-COCO dataset [13] using Lumina-mGPT [14] and Emu3 [27]. As shown in Fig. 5, images produced by our method (labeled w/ SJD-PAC) are visually indistinguishable from those generated by the original models. SJD-PAC drastically reduces decoding steps while strictly maintaining high-fidelity details.



Figure 6. Qualitative comparison with lossy acceleration.

In contrast, while lossy acceleration methods such as GSD [19] perform well in simple scenarios (Fig. 6, top row), they introduce noticeable artifacts due to the loss of high-frequency information (bottom row). This highlights the necessity of a lossless approach for preserving fine-grained details during complex image generation.

6. Conclusion

In this work, we introduced SJD-PAC, a novel and strictly lossless framework that directly addresses the inefficiencies of SJD [22] through two synergistic mechanisms. First, Proactive Drafting (PD) mitigates frequent single-token acceptance failures by proactively constructing a K -ary tree of diverse proposal paths immediately following a rejection, thereby increasing the probability of a valid draft in the subsequent iteration. Second, Adaptive Continuation (AC) refines the SJD verification loop. By continuing verification past the initial mismatch and resampling only the rejected tokens, AC preserves the stability of the sequence tail.

Our experiments demonstrate that SJD-PAC establishes a new state-of-the-art for training-free, lossless T2I acceleration. The combination of PD and AC reshapes the acceptance distribution, shifting its mass from inefficient short runs to highly efficient long ones. This synergy culminates in a $4.51\times$ step compression and a $3.80\times$ wall-clock speedup on Lumina-mGPT [14]. Notably, SJD-PAC achieves acceleration competitive with, or even superior to, several prominent lossy methods [17, 19, 23], proving that substantial speedups in T2I synthesis do not require compromising image fidelity.

While SJD-PAC is model-agnostic, its performance gains rely on a delicate empirical balance between the Proactive Drafting parameters (K , D) and the window length (L). Future work will explore integrating our framework with orthogonal approaches. Because SJD-PAC optimizes the drafting and verification processes, pairing it with methods that optimize the acceptance criterion, such as GSD [19], offers a promising direction. A hybrid approach combining our stable, multi-draft verification with advanced acceptance heuristics could push the boundaries of T2I model acceleration even further.

References

- [1] Ethan Chern, Jiadi Su, Yan Ma, and Pengfei Liu. Anole: An open, autoregressive, native large multimodal models for interleaved image-text generation. *arXiv preprint arXiv:2407.06135*, 2024. 1, 2
- [2] Chaorui Deng, Deyao Zhu, Kunchang Li, Chenhui Gou, Feng Li, Zeyu Wang, Shu Zhong, Weihao Yu, Xiaonan Nie, Ziang Song, et al. Emerging properties in unified multimodal pretraining. *arXiv preprint arXiv:2505.14683*, 2025. 1, 2
- [3] Patrick Esser, Robin Rombach, and Bjorn Ommer. Taming transformers for high-resolution image synthesis. In *Proceedings of the IEEE/CVF conference on computer vision and pattern recognition*, pages 12873–12882, 2021. 1
- [4] Maurice Fréchet. Sur la distance de deux lois de probabilité. In *Annales de l'ISUP*, pages 183–198, 1957. 5, 6
- [5] Google Research. Partiprompts benchmark. <https://parti.research.google/>, 2022. 5, 6
- [6] Jack Hessel, Ari Holtzman, Maxwell Forbes, Ronan Le Bras, and Yejin Choi. Clipscore: A reference-free evaluation metric for image captioning. In *Proceedings of the 2021 conference on empirical methods in natural language processing*, pages 7514–7528, 2021. 6
- [7] Martin Heusel, Hubert Ramsauer, Thomas Unterthiner, Bernhard Nessler, and Sepp Hochreiter. Gans trained by a two time-scale update rule converge to a local nash equilibrium. *Advances in neural information processing systems*, 30, 2017. 6
- [8] Gabriel Ilharco, Mitchell Wortsman, Nicholas Carlini, Rohan Taori, Achal Dave, Vaishaal Shankar, Hongseok Namkoong, John Miller, Hannaneh Hajishirzi, Ali Farhadi, et al. Openclip. *Zenodo*, 2021. 6
- [9] Doohyuk Jang, Sihwan Park, June Yong Yang, Yeonsung Jung, Jihun Yun, Souvik Kundu, Sung-Yub Kim, and Eunho Yang. Lantern: Accelerating visual autoregressive models with relaxed speculative decoding. *arXiv preprint arXiv:2410.03355*, 2024. 1, 3, 6
- [10] Jialiang Kang, Han Shu, Wenshuo Li, Yingjie Zhai, and Xinghao Chen. Vispec: Accelerating vision-language models with vision-aware speculative decoding. *arXiv preprint arXiv:2509.15235*, 2025. 3
- [11] Yaron Leviathan, Matan Kalman, and Yossi Matias. Fast inference from transformers via speculative decoding. In *International Conference on Machine Learning*, pages 21184–21195. PMLR, 2023. 1, 2
- [12] Yuhui Li, Fangyun Wei, Chao Zhang, and Hongyang Zhang. Eagle-2: Faster inference of language models with dynamic draft trees. In *Proceedings of the 2024 Conference on Empirical Methods in Natural Language Processing*, pages 7421–7432, 2024. 1, 5, 6, 7
- [13] Tsung-Yi Lin, Michael Maire, Serge Belongie, Ja Hays, Pietro Perona, Deva Ramanan, Piotr Dollár, and C Lawrence Zitnick. Microsoft coco: Common objects in context. In *European conference on computer vision*, pages 740–755. Springer, 2014. 4, 5, 6, 8
- [14] Dongyang Liu, Shitian Zhao, Le Zhuo, Weifeng Lin, Yi Xin, Xinyue Li, Qi Qin, Yu Qiao, Hongsheng Li, and Peng Gao. Lumina-mgpt: Illuminate flexible photorealistic text-to-image generation with multimodal generative pretraining. *arXiv preprint arXiv:2408.02657*, 2024. 1, 2, 4, 5, 6, 7, 8
- [15] Xupeng Miao, Gabriele Oliaro, Zhihao Zhang, Xinhao Cheng, Zeyu Wang, Zhengxin Zhang, Rae Ying Yee Wong, Alan Zhu, Lijie Yang, Xiaoxiang Shi, et al. Specinfer: Accelerating large language model serving with tree-based speculative inference and verification. In *Proceedings of the 29th ACM International Conference on Architectural Support for Programming Languages and Operating Systems, Volume 3*, pages 932–949, 2024. 3, 4
- [16] Siru Ouyang, Shuohang Wang, Minhao Jiang, Ming Zhong, Donghan Yu, Jiawei Han, and Yelong Shen. Temperature-centric investigation of speculative decoding with knowledge distillation. In *Findings of the Association for Computational Linguistics: EMNLP 2024*, pages 13125–13137, 2024. 1
- [17] Sihwan Park, Doohyuk Jang, Sungyub Kim, Souvik Kundu, and Eunho Yang. Lantern++: Enhancing relaxed speculative decoding with static tree drafting for visual auto-regressive models. *arXiv preprint arXiv:2502.06352*, 2025. 1, 3, 5, 6, 7, 8
- [18] Aditya Rah, Mikhail Pavlov, Gabriel Goh, Scott Gray, Chelsea Voss, Alec Radford, Mark Chen, and Ilya Sutskever. Zero-shot text-to-image generation. In *International conference on machine learning*, pages 8821–8831. Pmlr, 2021. 1, 2
- [19] Junhyuk So, Juncheol Shin, Hyunho Kook, and Eunhyeok Park. Grouped speculative decoding for autoregressive image generation. In *Proceedings of the IEEE/CVF International Conference on Computer Vision*, pages 15375–15384, 2025. 2, 3, 5, 6, 7, 8
- [20] Ziteng Sun, Ananda Theertha Suresh, Jae Hun Ro, Ahmad Beirami, Himanshu Jain, and Felix Yu. Spectr: Fast speculative decoding via optimal transport. *Advances in Neural Information Processing Systems*, 36:30222–30242, 2023. 5
- [21] Chameleon Team. Chameleon: Mixed-modal early-fusion foundation models. *arXiv preprint arXiv:2405.09818*, 2024. 1, 2
- [22] Yao Teng, Han Shi, Xian Liu, Xuefei Ning, Guohao Dai, Yu Wang, Zhenguo Li, and Xihui Liu. Accelerating autoregressive text-to-image generation with training-free speculative jacobi decoding. *arXiv preprint arXiv:2410.01699*, 2024. 1, 2, 3, 4, 5, 6, 7, 8
- [23] Yao Teng, Fuyun Wang, Xian Liu, Zhekai Chen, Han Shi, Yu Wang, Zhenguo Li, Weiyang Liu, Difan Zou, and Xihui Liu. Speculative jacobi-denoising decoding for accelerating autoregressive text-to-image generation. *arXiv preprint arXiv:2510.08994*, 2025. 2, 3, 5, 6, 7, 8
- [24] Aaron Van Den Oord, Oriol Vinyals, et al. Neural discrete representation learning. *Advances in neural information processing systems*, 30, 2017. 2
- [25] Ashish Vaswani, Noam Shazeer, Niki Parmar, Jakob Uszkoreit, Llion Jones, Aidan N Gomez, Łukasz Kaiser, and Illia Polosukhin. Attention is all you need. *Advances in neural information processing systems*, 30, 2017. 2
- [26] John Von Neumann et al. Various techniques used in connection with random digits. *John von Neumann, Collected Works*, 5:768–770, 1963. 3

- [27] Xinlong Wang, Xiaosong Zhang, Zhengxiong Luo, Quan Sun, Yufeng Cui, Jinsheng Wang, Fan Zhang, Yueze Wang, Zhen Li, Qiyang Yu, et al. Emu3: Next-token prediction is all you need. *arXiv preprint arXiv:2409.18869*, 2024. [1](#), [2](#), [5](#), [6](#), [7](#), [8](#)
- [28] Chengyue Wu, Xiaokang Chen, Zhiyu Wu, Yiyang Ma, Xingchao Liu, Zizheng Pan, Wen Liu, Zhenda Xie, Xingkai Yu, Chong Ruan, et al. Janus: Decoupling visual encoding for unified multimodal understanding and generation. In *Proceedings of the Computer Vision and Pattern Recognition Conference*, pages 12966–12977, 2025.
- [29] Yi Xin, Juncheng Yan, Qi Qin, Zhen Li, Dongyang Liu, Shicheng Li, Victor Shea-Jay Huang, Yupeng Zhou, Renrui Zhang, Le Zhuo, et al. Lumina-mgpt 2.0: Stand-alone autoregressive image modeling. *arXiv preprint arXiv:2507.17801*, 2025. [2](#)
- [30] Jiahui Yu, Yuanzhong Xu, Jing Yu Koh, Thang Luong, Gungjan Baid, Zirui Wang, Vijay Vasudevan, Alexander Ku, Yinfei Yang, Burcu Karagol Ayan, et al. Scaling autoregressive models for content-rich text-to-image generation. *arXiv preprint arXiv:2206.10789*, 2(3):5, 2022. [1](#), [2](#)
- [31] Guohui Zhang, Hu Yu, Xiaoxiao Ma, JingHao Zhang, Yaning Pan, Mingde Yao, Jie Xiao, Linjiang Huang, and Feng Zhao. Group critical-token policy optimization for autoregressive image generation. *arXiv preprint arXiv:2509.22485*, 2025. [1](#)

SJD-PAC: Accelerating Speculative Jacobi Decoding via Proactive Drafting and Adaptive Continuation

Supplementary Material

A. Proofs of Correctness

In this section, we provide the theoretical guarantee that SJD-PAC is lossless. That is, the distribution of the generated sequence converges exactly to the target distribution $p(x)$, identical to standard autoregressive sampling. We prove this by demonstrating that neither Adaptive Continuation (AC) nor Proactive Drafting (PD) introduces bias into the verified sequence.

A.1. Preliminaries

Let $p(x_i | x_{<i})$ denote the target distribution at position i given prefix $x_{<i}$, and $q(x_i | x_{<i})$ denote the draft distribution. Standard speculative decoding relies on the property that for a random variable X sampled via the rejection sampling scheme:

$$\begin{aligned} P(X = x) &= q(x) \cdot \min\left(1, \frac{p(x)}{q(x)}\right) \\ &\quad + \mathcal{N} \cdot \frac{\max(0, p(x) - q(x))}{\mathcal{N}} \quad (1) \\ &= p(x), \end{aligned}$$

where $\mathcal{N} = \sum_z \max(0, p(z) - q(z))$ is the normalization factor for the residual distribution. We refer to this standard result as the **Rejection Sampling Lemma**.

A.2. Proof of Correctness for Adaptive Continuation (AC)

Theorem 1. *AC preserves the target distribution $p(x)$ for all tokens accepted in the subsequent iteration.*

Proof. Let X^t denote the draft sequence generated by the AC mechanism during iteration t . At iteration $t + 1$, we verify the draft tokens x_j^t against the target distribution $p(x) = p(x | X_{<j}^{t+1})$. Let $q(x)$ denote the distribution used to generate the draft token at iteration t . Although q may be derived from stale context, it is fixed and known during the verification at $t + 1$.

To prove that the marginal probability of outputting a token matches the target distribution $p(x)$, we analyze the rejection sampling mechanism step-by-step. The probability of outputting a specific token x is the sum of the probability of it being accepted from the draft and the probability of it being resampled after a rejection.

Let $P(X_j^{t+1} = x)$ be the total probability that token x is generated at position j . We express this as:

$$P(X_j^{t+1} = x) = P(\text{Acc. } x) + P(\text{Rej.}) \cdot P(\text{Resamp. } x) \quad (2)$$

Probability of Acceptance: The draft proposes x with probability $q(x)$. The acceptance probability is defined as $\alpha(x) = \min\left(1, \frac{p(x)}{q(x)}\right)$. Thus, the joint probability of proposing and accepting x is:

$$\begin{aligned} P(\text{Acc. } x) &= q(x) \cdot \min\left(1, \frac{p(x)}{q(x)}\right) \quad (3) \\ &= \min\left(q(x), p(x)\right). \end{aligned}$$

Probability of Rejection. The probability of rejecting the draft (summing over all possible vocabulary tokens v) corresponds to the probability mass where the draft exceeds the target (or conversely, the missing mass):

$$\begin{aligned} P(\text{Rej.}) &= 1 - \sum_{v \in V} P(\text{Acc. } v) \\ &= \sum_{v \in V} p(v) - \sum_{v \in V} \min\left(q(v), p(v)\right) \quad (4) \\ &= \sum_{v \in V} \left(p(v) - \min\left(q(v), p(v)\right)\right) \\ &= \sum_{v \in V} \max\left(0, p(v) - q(v)\right). \end{aligned}$$

Probability of Resampling. Upon rejection, we sample from the residual distribution $p_{\text{res}}(x)$. This distribution is defined as the normalized difference between the target and the draft:

$$\begin{aligned} P(\text{Resamp. } x) &= p_{\text{res}}(x) \\ &= \frac{\max\left(0, p(x) - q(x)\right)}{\sum_{v \in V} \max\left(0, p(v) - q(v)\right)}. \quad (5) \end{aligned}$$

Observe that the denominator is the normalization constant, which equals $P(\text{Rej.})$ derived in Eq. (4).

Combining terms. Substituting these back into Eq. (2) for total probability:

$$\begin{aligned} P(X_j^{t+1} = x) &= \min\left(q(x), p(x)\right) \\ &\quad + P(\text{Rej.}) \frac{\max\left(0, p(x) - q(x)\right)}{P(\text{Rej.})} \quad (6) \\ &= \min\left(q(x), p(x)\right) \\ &\quad + \max\left(0, p(x) - q(x)\right) \end{aligned}$$

We consider two cases to solve this summation for any token x :

- **Case 1**, $p(x) \geq q(x)$:
 $\min(q(x), p(x)) + \max(0, p(x) - q(x)) = q(x) + (p(x) - q(x)) = p(x)$.
- **Case 2**, $p(x) < q(x)$:
 $\min(q(x), p(x)) + \max(0, p(x) - q(x)) = p(x) + 0 = p(x)$.

In both cases, the marginal probability $P(X_j^{t+1} = x)$ is exactly $p(x)$. Crucially, this equality holds independently of the quality or parameters of the draft distribution $q(x)$, provided that $q(x)$ is a valid probability distribution over the vocabulary. \square

A.3. Proof of Correctness for Proactive Drafting (PD)

Theorem 2. *PD, which involves the sequential verification of K candidates sampled without replacement and is supplemented by sampling from the residual distribution upon total rejection, guarantees exact recovery of the target distribution $p(x)$.*

Proof. We prove this theorem by induction on the number of candidates K .

Definitions. Let $p(x)$ denote the target probability distribution and $q(x)$ denote the draft distribution. PD generates a set of candidates by sampling iteratively from q without replacement. For the k -th candidate c_k , let $q^{(k)}(x)$ be the draft distribution adjusted for previous samples $\mathcal{C}_{<k} = \{c_1, \dots, c_{k-1}\}$, and $p^{(k)}(x)$ be the residual target distribution after previous rejections (with $p^{(1)} = p$). The adjusted draft distribution is:

$$q^{(k)}(x) = \begin{cases} \frac{q(x)}{1 - \sum_{y \in \mathcal{C}_{<k}} q(y)} & \text{if } x \notin \mathcal{C}_{<k} \\ 0 & \text{if } x \in \mathcal{C}_{<k} \end{cases} \quad (7)$$

The residual transition follows the Rejection Sampling Lemma established in Eq. (1):

$$p^{(k+1)}(x) = \frac{\max(0, p^{(k)}(x) - q^{(k)}(x))}{\sum_v \max(0, p^{(k)}(v) - q^{(k)}(v))}. \quad (8)$$

Base Case ($K = 0$). No candidates are proposed. The algorithm samples directly from the residual $p^{(1)}$, which is initialized as $p^{(1)} = p$. The output distribution is trivially correct.

Inductive Step. Assume that at step k , the target distribution is correctly captured by the residual $p^{(k)}$. We verify that the procedure at step k preserves this distribution.

Specifically, the probability of rejecting candidate c_k is the complement of the acceptance mass:

$$\begin{aligned} P(\text{Rej. } c_k) &= \sum_x q^{(k)}(x) \left(1 - \min \left(1, \frac{p^{(k)}(x)}{q^{(k)}(x)} \right) \right) \\ &= \sum_x \max \left(0, p^{(k)}(x) - q^{(k)}(x) \right). \end{aligned} \quad (9)$$

We now show that the marginal probability of accepting a token u at step k , or rejecting it and subsequently sampling it from the next residual $p^{(k+1)}$, equals the probability of sampling u from the current target $p^{(k)}$.

$$\begin{aligned} p^{(k)}(u) &\stackrel{?}{=} \underbrace{q^{(k)}(u) \cdot \min \left(1, \frac{p^{(k)}(u)}{q^{(k)}(u)} \right)}_{\text{Accept } u \text{ at step } k} \\ &\quad + \underbrace{P(\text{Rej. } c_k) \cdot p^{(k+1)}(u)}_{\text{Sample } u \text{ from residual}} \end{aligned} \quad (10)$$

Substituting the definition of $p^{(k+1)}(u)$ and the rejection probability from Eq. (9):

$$\begin{aligned} \text{RHS} &= \min \left(q^{(k)}(u), p^{(k)}(u) \right) \\ &\quad + p^{(k+1)}(u) \sum_x \max \left(0, p^{(k)}(x) - q^{(k)}(x) \right) \\ &= \min \left(q^{(k)}(u), p^{(k)}(u) \right) \\ &\quad + \frac{\max(0, p^{(k)}(u) - q^{(k)}(u))}{\sum_x \dots} \sum_x \dots \\ &= \min \left(q^{(k)}(u), p^{(k)}(u) \right) \\ &\quad + \max \left(0, p^{(k)}(u) - q^{(k)}(u) \right) \\ &= p^{(k)}(u). \end{aligned} \quad (11)$$

By induction, since the procedure preserves the target distribution at each step k , and the final sampling upon total rejection is drawn from $p^{(K+1)}$, the overall Proactive Drafting process exactly recovers $p(x)$. \square

B. Overhead Analysis

In this section, we analyze the memory consumption and computational latency introduced by SJD-PAC compared to the vanilla AR baseline.

GPU Memory Consumption. We evaluate the memory footprint on Lumina-mGPT [14]. The baseline implementation requires approximately 18.7 GB of GPU memory. Implementing SJD-PAC with a decoding window length of $L = 64$ results in a memory usage of 18.7 GB, demonstrating negligible memory overhead.

Although SJD-PAC employs a significantly larger decoding window ($L = 64$) compared to vanilla AR ($L = 1$), the memory cost remains stable. This is because the KV cache is inherently required to store the history of the generated sequence. In our approach, the accepted tokens within the window are immediately converted into persistent KV cache entries. Consequently, the memory used by the window effectively acts as pre-allocated space for the upcoming KV cache, rather than an add-on burden.

Computational Latency. We break down the runtime costs per step to analyze the temporal overhead. The breakdown is summarized in Tab. 4. For the vanilla AR model, a single forward pass takes approximately 40.8 ms, with miscellaneous overheads totaling roughly 1.0 ms. With SJD-PAC ($L = 64$), the model forward pass increases slightly to 44.3 ms. The additional components specific to our algorithm include tree verification and generation (3.2 ms) and KV cache maintenance (2.2 ms).

Table 4. Runtime breakdown of a single decoding step in milliseconds. Comparison between Vanilla AR and SJD-PAC with window length $L = 64$.

Operation	Vanilla AR SJD-PAC	
Model Forward	40.8 ms	44.3 ms
Tree Verification & Generation	-	3.2 ms
KV Cache Update & Backtracking	-	2.2 ms
Other Overheads	1.0 ms	1.0 ms

Despite the overhead of SJD-PAC, verification is efficient due to the high parallelizability enabled by the static tree structure and independent positional operations. Moreover, as current KV cache overheads arise mainly from non-contiguous memory access, future optimizations for contiguous layouts are expected to further mitigate latency.